The oxidative stability of carbon fibre reinforced glass-matrix composites

K. M. PREWO, J. A, BATT
United Technologies Research Center, East Hartford, Connecticut 06108, USA

The environmental stability of carbon fibre reinforced glass-matrix composites is assessed. Loss of composite strength due to oxidative exposure at elevated temperatures under no load, static load and cyclic fatigue as well as due to thermal cycling are all examined. It is determined that strength loss is gradual and predictable based on the oxidation of carbon fibres. The glass matrix was not found to prevent this degradation but simply to limit it to a gradual process progressing from the composite surfaces inward.

1. Introduction
Current carbon fibre reinforced resin-matrix composites are limited in their maximum use temperature by the instability of their matrices. Through the use of glass as a matrix much higher application temperatures are possible. The earliest development of carbon fibre reinforced glass demonstrated the system's excellent toughness and strength [1-9] while more recent development has also emphasized the ability to achieve composites with dimensional stability [10, 11] and wear resistance [12, 13].

The purpose of this study was to examine the resistance of carbon fibre reinforced glass composites to oxidation in both unstressed and stressed conditions.

2. Experimental procedure
All composites were fabricated using a borosilicate glass powder (Corning Glass Works, New York designation 7740) and high modulus carbon fibres (Hercules HM, Magna, Utah, USA). Fibre properties were an elastic modulus of 350 GPa and a tensile strength of 2700 MPa.

Composite fabrication consisted, in all cases, of first making a precursor tape of fibre and dispersed glass powder. This tape was then cut into segments and placed in graphite dies for hot-press consolidation into composite panels [8, 14].

All composites were unidirectionally reinforced and contained 50 to 60 vol % of fibres with less than 2% matrix porosity. The overall composite density was approximately $2.0 \, \text{g cm}^{-3}$. Samples were cut from these panels to dimensions of $0.2 \, \text{cm} \times 0.5 \, \text{cm} \times 7.7 \, \text{cm}$ with the 7.7 cm dimension parallel to the 0° fibre direction. All specimen surfaces were diamond-ground to remove any excess glass and expose the composite interior microstructure. For thermal exposure testing some samples were left with their ends (surfaces containing the fibre ends) coated with excess glass to determine whether this inhibited oxidation along the fibre axes.

All mechanical tests were performed in the three-point flexural mode with a span-to-depth ratio of approximately 25. All specimens were oriented with the 0° fibre axis along the major span of test. Except where noted, all elevated-temperature tests and exposures were in static furnace air.

3. Results and discussion
3.1. Unstressed thermal exposure - constant temperature
The change in mass of unidirectionally reinforced borosilicate glass matrix composites is given in Fig. 1 as a function of exposure time to air at the indicated temperatures. It was found that the total loss of mass after even 500 h at 430° C was less than 5%, while a similar length of exposure to 540° C resulted in 30 to 50% mass reduction. As shown in Fig. 1, there was very little dependence of performance on whether the specimen ends were glass-rich (untrimmed ends) or whether the ends were trimmed to remove any excess glass.

After measurement of their residual mass several of the exposed specimens were tested to failure in three-point bend to measure their flexural strength (Fig. 2). As would be expected from the data for change in mass, the composite strength was significantly reduced after exposure at 540° C. To get a better understanding of this and the mechanisms which control composite mass and strength loss, several specimens were sectioned and polished. The examination of both transverse and longitudinal sections taken from exposed composites revealed two distinctly different rate processes taking place, one from the sides (transverse) and one from the specimen ends inward. Fig. 3 represents the results obtained by sectioning several different exposed samples and measuring the transverse depth of oxidation as seen by the loss of carbon fibres. In the figure, the shaded regions are those in which oxidative loss of carbon fibres was observed while the lighter central regions appeared undegraded. These transverse sections were taken near the centres of the exposed samples to avoid any confusion with oxidation taking place from the specimen ends, and all of the specimen surfaces had been ground prior to exposure to remove any excess glass.
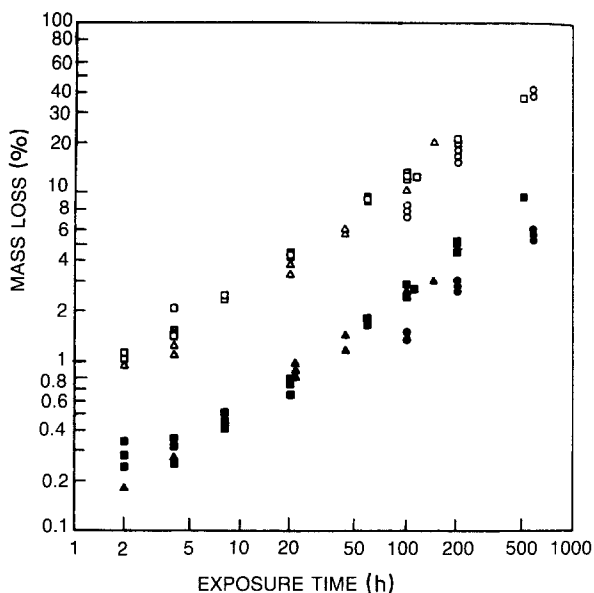
As can be seen from the cross-sections in Fig. 3, the

Figure 1 Change in composite mass as a function of exposure time in air. (O, ●) To be flex-tested; (△, ▲) with trimmed ends; (□, ■) with untrimmed ends. Open symbols, 540° C; closed symbols, 430° C.

oxidation process proceeded on both a broad front and also along preferred paths. The latter were frequently, but not always, associated with glass-rich regions which existed between adjacent bundles of fibres. The fibres adjacent to these glass-rich regions appeared to be oxidized more rapidly than those within the bundles themselves. The higher rate of oxidation at the glass-rich boundaries was probably due to the presence of cracks in these regions which were created during composite cool-down from the composite fabrication temperature. Sections like those shown in Fig. 3 were used to obtain average values of transverse oxidation penetration depth to plot as a function of exposure time, (Fig. 4). Each value of average depth was arrived at by measuring the total area of oxidized material in a given specimen section and dividing this area by the original specimen cross-sectional surface length, i.e. twice the sum of thickness plus width.

It was found, using similar procedures, that the rate of oxidation in the longitudinal direction (parallel to the fibres) was much more rapid than that in the transverse direction, (Fig. 4). It also progressed in a non-uniform manner (Fig. 5), although in this case the
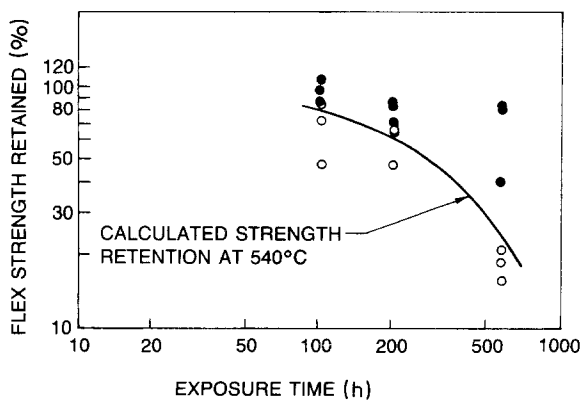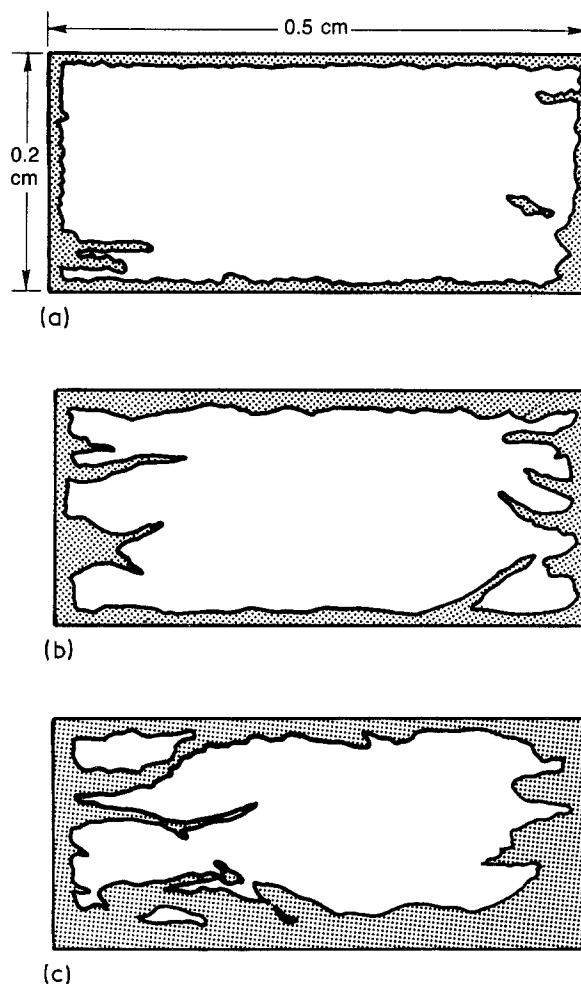

Figure 3 Schematic representations of transverse sections of composite after exposure to air at 540° C for (a) 100 h, (b) 147 h and (c) 500 h. The shaded regions are those in which the carbon fibres have been oxidized.
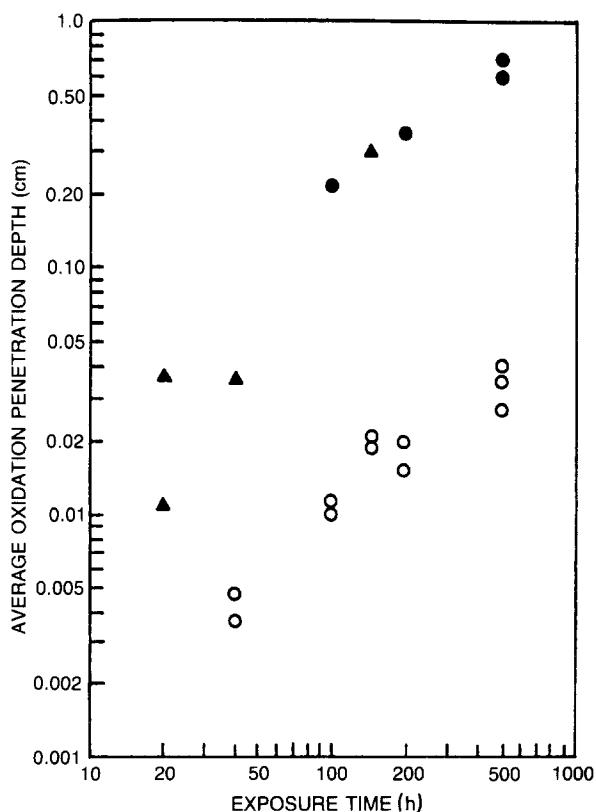

Figure 2 Change in 22° C flexural strength as a function of exposure time in air. (O) 540° C, (●) 430° C.

Figure 4 Average depth of oxidation penetration as a function of exposure time to air at 540° C. (●) d_L, glass-rich ends; (▲) d_L, trimmed ends; (O) d_T.
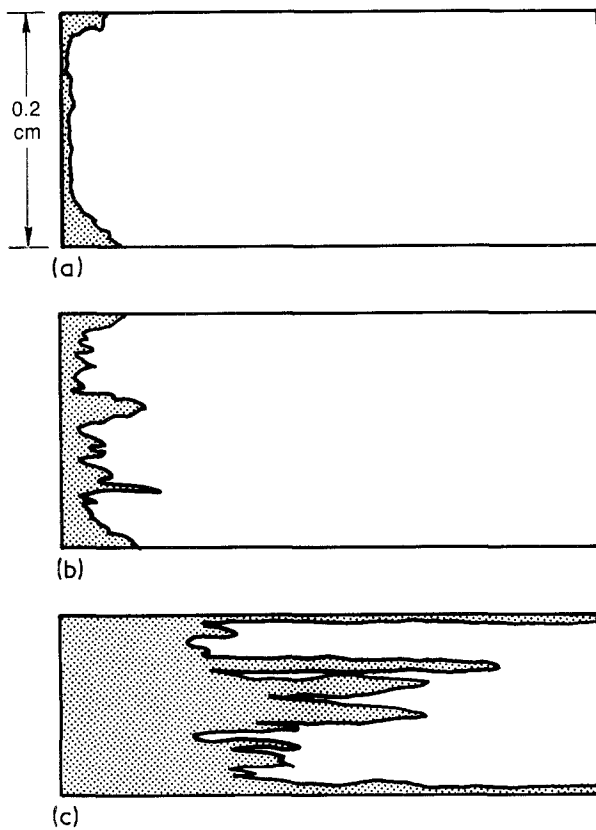
524

(a)

0.2 cm

(b)

(c)

Figure 5 Schematic representations of longitudinal sections of composite after exposure to air at 540°C for (a) 20 h, (b) 40 h and (c) 147 h. The shaded regions are those in which the carbon fibres have been oxidized.

Figure 6 Comparison of calculated and measured percentage mass loss for specimens oxidized at 540°C in air. (O) Total calculated mass loss, (△) calculated transverse mass loss, (□) calculated longitudinal mass loss.

nature of the preferential paths of attack was not discernable. Specimens with both glass-rich ends and with ends that had been machined to remove any excess glass were both tested. It was found that the glass coating, left on the specimen ends as a result of fabrication, was not protective. Note that for the glass-rich specimen ends the depth of penetration was taken relative to the initial ends of the fibres inward and not from the outside glass surfaces of the specimens.

By use of the data in Fig. 4 is was possible to calculate the contributions to specimen mass loss due to both transverse and longitudinal penetration. The total percentage mass loss can be calculated using the formula

$$\% \text{ mass loss} = \frac{\varrho_F(v/oF)\,(d_L A_L + d_T A_T)}{W_c}$$

where ϱ_F = density of the fibre, v/oF = the volume percentage of fibre in the composite, d_L, d_T = longitudinal and transverse depth of penetration, respectively, A_L, A_T = longitudinal and transverse original specimen surface areas, respectively and W_c = original unoxidized mass of the composite.

The resultant total calculated mass loss, as well as the individual longitudinal and transverse contributions, are presented in Fig. 6. The range of measured composite mass loss is also plotted in the figure and it can be seen that the calculated and measured values agree quite well. It is also interesting to note that, although the rate of oxidation is much more rapid from the specimen ends, the relatively small specimen-
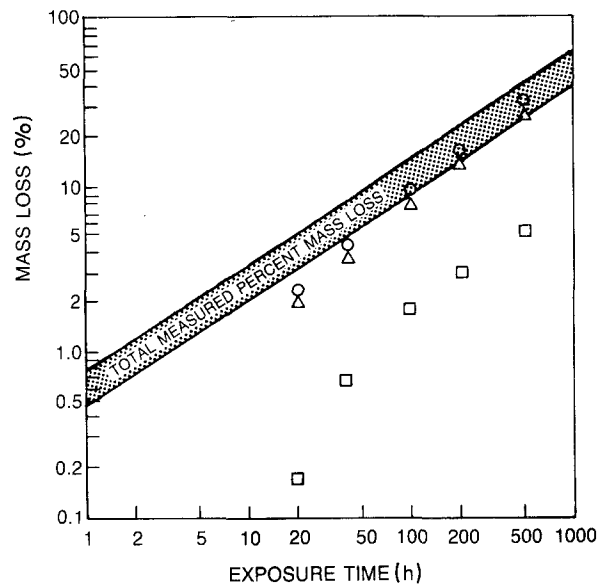
end surface area causes this path to be the minor contributor to total specimen mass loss.

An attempt has also been made to calculate the expected rate of composite flexural strength loss due to oxidation. This has been accomplished by assuming that strength loss is due to a simple reduction in composite beam transverse cross-section and that the effects of non-uniform transverse attack are unimportant. The calculation was put in the following form to result in a measure of the percentage flexural strength retained:

% flexural strength retained

$$= \frac{100(b - 2d_T)\,(h - 2d_T)^2}{bh^2}$$

where b, h = the original unexposed specimen width and depth, respectively.

This formula stems from the ratio of three-point bend flexural strengths of exposed and unexposed specimens. A curve representing the calculated levels of strength retention is presented in Fig. 2 along with the originally measured data discussed previously. The level of agreement substantiates the postulated mechanism and indicates that there are no major additional degrading effects due to a notch sensitivity or the occasional deeply penetrating regions of degradation.

3.2. Unstressed thermal exposure – cyclic temperature

The results obtained by thermally cycling specimens were rather similar in form to those obtained by static thermal exposure. HM fibre-reinforced composites exhibited a gradual mass loss with increasing number of cycles and this mass loss caused a measurable decrease in composite flexural strength (Fig. 7). In the case of thermal cycling to 540°C, examination of the thermal history which took place during each cycle made it possible to judge that 1000 cycles corresponded to approximately 75 h at 540°C. The 70 to 85%
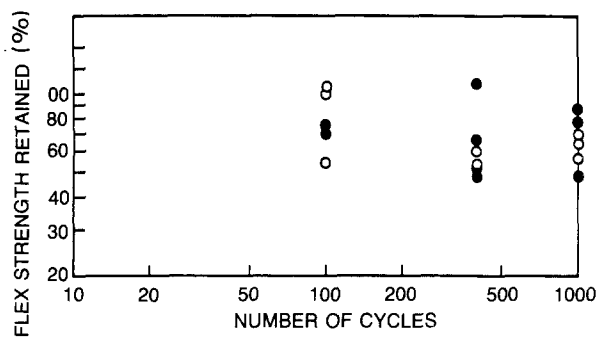
525

Figure 7 Change in flexural strength as a function of the number of thermal cycles in air. Maximum temperature (O) 540° C, (●) 430° C.

TABLE I 22°C flexural strength of unexposed and stress-rupture-tested specimens

Exposure condition	Flexural strength after exposure (MPa)
None	634
None	638
None	992
None	1081
None	1085
None	1102
200 h, 560 MPa	943
200 h, 597 MPa	795
200 h, 636 MPa	799

strength retention after 1000 cycles (Fig. 7) is in good agreement with the level of strength retained after 100 h of constant temperature exposure (Fig. 2).

3.3. Thermal exposure under constant stress

Specimens were loaded in three-point bend and held under constant stress for prolonged periods of up to 200 h. The resultant times to rupture against the applied maximum flexural stresses are presented in Fig. 8. Shown on the figure are also the starting flexural strengths of specimens at room temperature (22° C) as a point of reference. It was found that all of the specimens tested at 540° C failed prior to the 200 h maximum exposure, while three of the 430° C tests resulted in specimens surviving. The residual strengths of these survivors were determined at room temperature and found to be within the range of strengths of the unexposed composites (Table I) and also within the strength range of specimens that were exposed in an unstressed condition.

To aid in this interpretation of the role of applied stress, Fig. 8 also includes data which indicate the residual composite strength obtained from specimens that were exposed to the temperatures indicated without any applied stress, i.e. data from Fig. 2. Thus, at 540° C it would appear that the application of stress accelerated composite degradation, and that specimen failures occurred at times and stress levels less than anticipated simply on an oxidative basis. At 430° C,

however, the stress rupture times extend into the residual strength band, indicating that the continuous application of stress was not important in degrading composite strength.

3.4. Thermal exposure under cyclic stress

Flexural fatigue tests were performed at a rate of three cycles per second. The minimum stress in each cycle was 10% of the maximum stress and tests were run for a maximum of 10^6 cycles at 22° and 430° C. The resultant data (Fig. 9) indicate that all of the fatigue conditions were chosen at stresses that occur within the population of initial composite 22° C strength (the points at 10^0 cycles indicate this strength range). One specimen at 22° C survived the full 10^6 cycles, while three samples at 430° C almost achieved full run-out which required approximately 100 h of testing. By comparison with the data in Fig. 8 it is apparent that mechanical fatigue at 430° C was no more severe in reducing composite strength than either unstressed or statically stressed conditions.

4. Summary

The carbon fibre reinforced glass system provides the opportunity to achieve composites whose use temperature is well above that of current polymer composites and at densities much less than metal-matrix composites. Through the use of high-performance carbon fibres, values of strength and stiffness can be
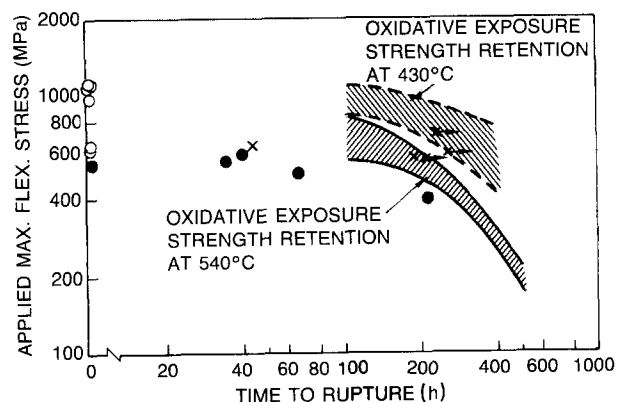

Figure 8 The data points are the results of experiments which determined the applied maximum flexural stress as a function of time to cause specimen fracture for specimens exposed to air under constant stress at elevated temperature. The shaded regions are taken from Fig. 2, representing the retention of strength for specimens exposed to oxidation under no applied stress. (O) 22° C, (x) 430° C, (●) 540° C, (x→) no failure.
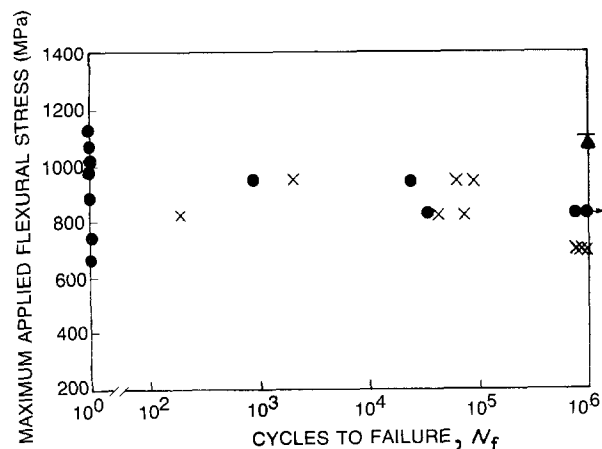

Figure 9 Applied maximum cyclic flexural stress as a function of number of cycles to cause specimen fracture for specimens fatigue-tested in air at 22 and 430° C. At 22° C: (●) specimen fracture, (●→) unfractured, (▲) residual flexural strength. At 430° C: (x) specimen fracture.
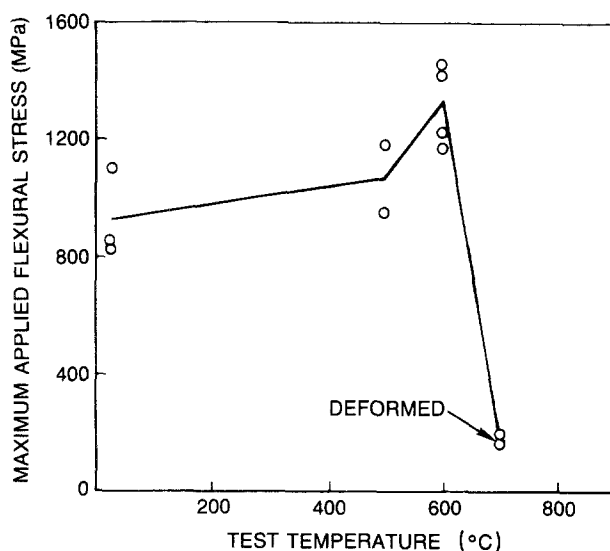
Figure 10 Flexural strength of specimens tested at temperature in an inert argon atmosphere.

achieved comparable to those of current carbon–epoxy systems. An example of the type of performance achievable is shown in Fig. 10 where composite three-point flexural strength is given as a function of test temperature for tests performed in the inert atmosphere of argon. The change in strength with temperature is caused by the change in performance of the borosilicate glass matrix. It begins to soften at above 500° C, and this causes a significant increase in observed flexural strength due to the enhanced ability to redistribute loads in the specimen. At 700° C, however, the matrix has softened sufficiently to cause the samples to simply deform extensively without any fracture occurring. Glass and glass–ceramic matrices with superior high-temperature performance can extend the range of composite strength retention to much higher temperatures [8], though only in an inert atmosphere. As shown by the data presented in the current paper, oxidative attack of the carbon fibres is a significant life-limiting mechanism. The glass matrix does prevent oxidative attack from occurring simultaneously throughout the composite body; however, it does not prevent a progressive deterioration propagating inward from the exterior surfaces. It has been shown that this loss of carbon is highly anisotropic, with attack occurring much more rapidly parallel to the fibres as compared with the transverse direction.

While this oxidative attack is significant it is important to note that it is gradual and does not cause a change in basic composite behaviour. The measured losses of strength can be simply associated with the gradual loss of carbon fibres due to oxidation. The surface regions of composite which experienced fibre loss did not act to embrittle or alter the performance of the remaining, unattacked, interior composite. Similarly, the application of both constant and cyclic stresses, at elevated temperatures in air, did not cause

a significantly increased rate of attack and loss of strength or change in failure mode. This is notably different than the behaviour of Nicalon-type silicon carbide yarn reinforced glass–ceramic-matrix composites, where the application of stress in air at elevated temperatures can cause a significant embrittlement in composite fracture mode [15, 16].

As a result of the observations that the strength loss is gradual, occurs at controlled rates from the exterior surfaces inward, and does not cause embrittlement of the remaining substrate composite, it can be concluded that strength loss for any application of this material will depend on the component size and configuration. For large, thick components the rate of observed strength loss will be significantly less than that observed in this study. For plates thinner than 0.2 cm the converse will be true.

Acknowledgement

References

1. I. CRIVELLI-VISCONTI and G. A. COOPER, *Nature* **221** (1969) 754.
2. R. A. SAMBELL, D. BOWEN and D. C. PHILLIPS, *J. Mater. Sci.,* **7** (1972) 663.
3. R. A. SAMBELL, A. BRIGGS, D. C. PHILLIPS and D. H. BOWEN, *ibid.* **7** (1972) 676.
4. D. C. PHILLIPS, R. A. SAMBELL and D.H. BOWEN, *ibid.* **7** (1972) 1454.
5. K. M. PREWO and J. F. BACON, in Proceedings of 2nd International Conference on Composites, Vol. 1, edited by B. Noton (AIME, New York, 1978) p. 64.
6. K. M. PREWO, *J. Mater. Sci.* **17** (1982) 3549.
7. K. M. PREWO, J. F. BACON and D. L. DICUS, *SAMPE Q.* **10** (4) (1979) 42.
8. K. M. PREWO and E. R. THOMPSON, "Research on Graphite Reinforced Glass Matrix Composites", NASA Contract Report 165711 (1981).
9. K. M. PREWO and E. J. MINFORD, *SAMPE J.* **21/2** (March 1985).
10. K. M. PREWO, in Proceedings of the Special Topics in Advanced Composites Meeting, El Segundo, California (Technical Conferences Inc., 1979) p. 1.
11. K. M. PREWO and E. J. MINFORD, *Proc. SPIE – Int. Soc. Opt. Engnrs.* **505** (August 1984).
12. V. D. KHANNA, Z. ELIEZER, J. McKITTRICK and M. F. AMATEAU, "Mechanical Behavior of Metal-Matrix Composites", edited by J. E. Hack and M. F. Amateau (AIME, Warrendale, P.A., 1983) p. 227.
13. E. MINFORD and K. PREWO, *Wear* **102** (1985) 253.
14. K. M. PREWO, J. J. BRENNAN and G. K. LAYDEN, *Ceram. Bull.* **65** (2) (1986) 305.
15. T. MAH, M. MENDIRATTA, A. KATZ, R. RUH and K. S. MAZDIYASNI, *J. Amer. Ceram. Soc.* **68** (9) (1985) C248.
16. K. M. PREWO, *J. Mater. Sci.* **21** (1986) 3590.